Nonlinear Dynamics and Systems Theory, **1**(2) (2001) 205–218

Chaotic Control Systems

T.L. Vincent

College of Engineering and Mines, Department of Aerospace and Mechanical Engineering, The University of Arizona, Tucson Arizona 85721, USA

Received: July 15, 2000; Revised: December 21, 2000

Abstract: Generally speaking, it is relatively easy to design a feedback controller to eliminate the possibility of chaos in a nonlinear dynamical system. Here we examine chaotic control not from the prospective of eliminating chaos, but from the prospective of producing chaotic motion in order to take advantage of the random like "free ride" a chaotic attractor provides. The idea is stay with this free ride until the system moves into a target containing a desired fixed point. Once inside this target, feedback control is applied that provides asymptotic stability for the fixed point. A basic requirement with this approach is to determine an appropriate target. It must be a subset of the domain of attraction to the fixed point under state variable feedback control. In addition, the target must be large enough so that the time it takes for the system to reach it, under chaotic control, is not unreasonably large. After addressing the question as to why this might be a desirable approach for nonlinear control system design, the focus of this paper is on the presentation of a general method for applying chaotic control and then demonstrating its use in controlling an inverted pendulum and a bouncing ball.

Keywords: *Chaos; control; inverted pendulum; bouncing ball.*

Mathematics Subject Classification (2000): 49J15, 70Q05, 93C15.

1 Introduction

The full potential of control system design is often overlooked since there exists a strong prejudice, in classical control text books, to only deal with linear systems. A major focus of control system design is to achieve asymptotic stability to an equilibrium point. Since nonlinear systems are generally "linearized" before applying linear control design methods, chaotic or other motion which can only occur in nonlinear systems is not generally considered to be a part of the design process. However, for years, controls engineers have been using traditional linear control methods to control systems which

have the potential for chaos. This is not thought of as "controlling chaos" as chaos or any motion other than asymptotic stability or tracking is suppressed.

Poincaré [1] noted in 1892 that certain mechanical systems could display chaotic motion. However the notion that deterministic models of discrete or continuous nonlinear dynamical systems could behave chaotically did not attract wide attention until Lorenz [2] in (1963), May [3] in (1976), and others reported chaotic behavior in very simple dynamical models.

In 1990, Ott, Grebogi and York [4] published the first paper to point out that chaos could be advantageous in achieving control objectives. Their method, now called the OGY method, involves stabilizing one of the unstable periodic orbits embedded in the chaotic attractor using small time dependent perturbations of a system parameter. Chaotic motion allows this method to work since all of the unstable periodic orbits will eventually be visited. One simply waits until the chaotic motion brings the system near a neighborhood of the proper unstable periodic orbit, at which time the small control is applied. Many variants of this method have appeared in the literature [5]. A more traditional control approach to regulating the Lorenz equations appeared in 1991 [6].

Since that time there have been a number of other papers dealing with the control of chaotic systems [7 – 12] including feedback control of the Lorenz equations [13, 14]. These references tend to focus on the problem of designing a stabilizing controller for systems which, without control, would be chaotic. However, since chaos can be useful in moving a system to various points in state space, the systems of interest here are not necessarily chaotic but as in [15 – 17] chaotic motion can be created as a part of the total control design. We make use of the fact that for many nonlinear systems chaos is easy to create using open-loop control. In particular, see [18] for a discussion of producing chaos in the driven pendulum system.

In the **chaotic control algorithm** given below, two essential ingredients are needed: a chaotic attractor and a controllable target. It is assumed that chaos can be created using open loop control. A **controllable target** is any subset of the domain of attraction to a equilibrium point, under a corresponding feedback control law, that has a nonempty intersection with the chaotic attractor. Thus the equilibrium point itself need not be on the chaotic attractor. If we start the system at any point within the basin of attraction of the chaotic attractor, the resulting chaotic motion will ultimately arrive in the controllable target. The chaotic control algorithm simply has to keep track of when the system enters the controllable target. When it does, the open loop control used to create chaos is turned off and at the same time the closed-loop feedback control is turned on.

The chaotic control algorithm has some distinct advantages in designing controllers for nonlinear systems. Its main advantage is simplicity. Consider for a moment one of the alternatives. Optimal control [19 – 21] is well suited for nonlinear problems and numerical methods are available [22] for solving complex problems. However optimal control solutions, for nonlinear problems, obtained by applying Pontryagin's maximum principle are generally open-loop. One could use this open-loop control to drive the system to a controllable target in a direct fashion. However such a control program would not be robust in the sense that if a perturbation were to drive the system outside of the controllable target, one could not simply turn the open loop control back on. The only alternative would be to start over again.

2 Stability under Chaotic Control

Consider the class of dynamical systems, subject to control, which can be described by either nonlinear difference equations of the form (discrete system)

$$\mathbf{X}_{(t+1)} = \mathbf{F}(\mathbf{X}, \mathbf{U}) \tag{2.1}$$

or nonlinear differential equations of the form (continuous system)

$$\dot{\mathbf{X}} = \mathbf{F}[\mathbf{X}, \mathbf{U}], \tag{2.2}$$

where $\mathbf{F} = [F_1 \cdots F_{N_X}]$ is an N_X dimensional vector function of the state vector $\mathbf{X} = [X_1 \cdots X_{N_X}]$, and control vector $\mathbf{U} = [U_1 \cdots U_{N_U}]$. Current time is indicated by t and the subscript $(t+1)$ is used to denote one time unit latter. The dot $(\dot{})$ denotes differentiation with respect to time. For the discrete system, t is just a counter and need not denote actual time. The functions F_i are assumed to be continuous and continuously differentiable in their arguments. The control will, in general, be bounded and it is assumed that at every time t, the control $\mathbf{U}$ must lie in a subset of the control space $\mathcal{U}$ defined by the inequalities

$$U_{i_{\min}} \leq U_i \leq U_{i_{\max}}$$

for $i = 1 \cdots N_U$.

The control input $\mathbf{U}$ is either a specified function of time, $\mathbf{U}(t)$ (open-loop) or a specified function of the state, $\mathbf{U}(\mathbf{x})$ (closed-loop). Assume that for all t there exists a specified open-loop control input $\widehat{\mathbf{U}}(t)$ such that the system has a chaotic attractor. Furthermore assume that for a specified constant control, $\widehat{\mathbf{U}}(t) \equiv \bar{\mathbf{U}}$, there is a corresponding fixed point of interest which is near the chaotic attractor. The fixed point satisfies

$$\bar{\mathbf{X}} = (\bar{\mathbf{X}}, \bar{\mathbf{U}})$$

for the discrete difference equation system and it satisfies

$$\mathbf{F}(\bar{\mathbf{X}}, \bar{\mathbf{U}}) = 0$$

for the continuous differential equation system.

Given the above assumptions, the controllable target is obtained using a method of linearization and Lyapunov function estimates [16, 21]. The nonlinear system is first linearized about the fixed point. The resulting linear system is assumed to be controllable and the LQR method [23, 24] is used to design a full state variable feedback controller that will guarantee the origin for this system is asymptotically stable. This, in turn, implies that for the nonlinear system, the fixed point will be asymptotically stable in some neighborhood containing the fixed point. An under estimate for this neighborhood is then determined using a Lyapunov function obtained from the linear system. This under estimate is used as the controllable target. Full details of this approach is given in [17]. We will now illustrate the application of this chaotic control method to two systems. The first is continuous and the second is discrete.

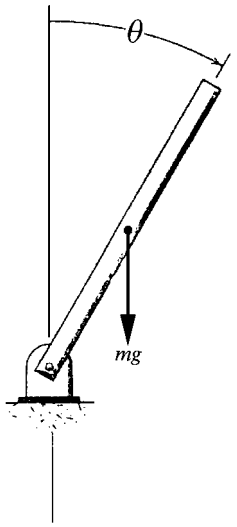

Figure 3.1. Inverted pendulum attached to a DC motor.

3 Inverted Pendulum

Consider the inverted pendulum, attached to a DC motor as shown in Figure 3.1. The pendulum is free to rotate through all angles so that it has stable downward equilibrium positions at $\theta = \pi(1 \pm 2n),\ (n = 0, 1, 2, \dots)$ and unstable upright equilibrium position at $\theta = 2n\pi,\ (n = 0, 1, 2, \dots)$. Let $x_1 = \pi - \theta$ be the angle of the pendulum as measured from the downward position, $\dot{x}_1$ be the rate of change of this angle, and bu be the torque applied by the motor. Positive values are in the counter clockwise direction. In terms of these variables, the equations of motion are given by

$$\begin{aligned} \dot{x}_1 &= x_2, \\ \dot{x}_2 &= a_1 \sin x_1 + a_2 x_2 + bu, \end{aligned} \tag{3.1}$$

where a_1, a_2, and b are constants associated with the system. The term $a_1 \sin x_1$ is the torque provided by gravity, $a_2 x_2$ is damping provided by friction and back EMF of the motor, bu is the control torque provided by a DC motor, and u is the voltage applied to the motor, with $|u| \le u_{\max}$. The particular system that we will examine here has [21]

$$\begin{aligned} a_1 &= -17.627 \text{ rad/sec}^2 \\ a_2 &= -0.187 \text{ sec}^{-2} \\ b &= 0.6455 \text{ rad/volt-sec}^2 \\ u_{\max} &= 18 \text{ volts}. \end{aligned}$$

Our objective is to stabilize the inverted pendulum in the vertical upright position.

If we linearize this system about $\bar{\mathbf{X}} = [\,\pi \quad 0\,]^{\mathrm{T}}$, then we can use LQR design [24] with $\mathbf{Q}$ and $\mathbf{R}$ identity matrices to obtain the feedback gains

$$\mathbf{K} = \begin{bmatrix} 54.6333 & 12.7624 \end{bmatrix},$$

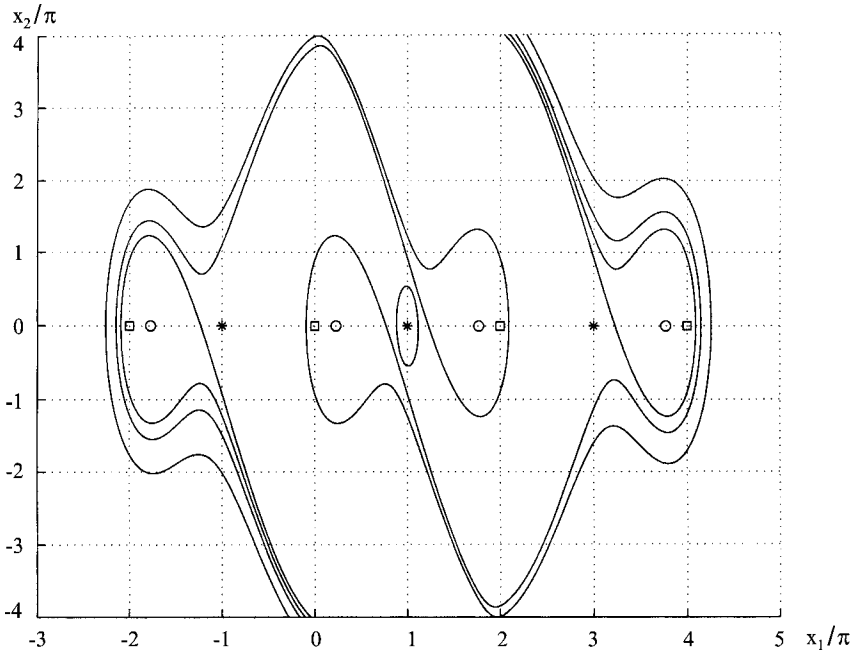

Figure 3.2. Domain of attraction for the inverted pendulum.

with the eigenvalues for the linearized controlled system given by $\lambda_1 = -4.5397$ and $\lambda_2 = -3.8855$. Under LQR design the feedback control law is given by

$$u(\mathbf{x}) = -\mathbf{K}(\mathbf{x} - \bar{\mathbf{X}}). \tag{3.2}$$

However since there are bounds on the control, the actual feedback control law used is that of saturating feedback control [21].

We can find the domain of attraction under saturating LQR control as applied to the nonlinear system (3.1) by integrating backward from points very close to the equilibrium points obtained when the control is set equal to $\pm u_{\max}$. The results are illustrated in Figure 3.2. In order to "see" the domain of attraction in this figure, first pinpoint the star located inside the ellipse. This represents $\bar{\mathbf{X}}$. The domain of attraction, to this point is the set of all points obtained by "flooding" with a color, from the star, or by drawing all continuous curves from the star which do not cross any of the curves contained in the figure other than the ellipse. Observe that, in places, the domain of attraction narrows down and becomes tubular.

Note that the x_1 and x_2 axis are in multiples of π. The equilibrium point $\bar{\mathbf{X}}$ and the first 2π multiple to the right and left are marked with a star, the squares locates stable equilibrium points, and the circles locate the equilibrium solutions obtained if saturating LQR control is used outside the domain of attraction.

Consider any one of the lob-like objects which contain a square and a small circle. If the system, under saturating LQR control is started anywhere inside the lob, including its tubular extension, it will remain in it, ultimately arriving at the equilibrium point contained in the lobe. Clearly these regions are not in the domain of attraction to $\bar{\mathbf{X}}$.

In fact, the domain of attraction to $\bar{\mathbf{X}}$ is simply all other points. Note that these other points include the stars located at 2π multiples of $\theta = 0$. Saturating LQR controller will not stabilize the system to these points since it does not recognize any vertical equilibrium position other than the one corresponding to $\theta = \dot{\theta} = 0$. In other words if the system were started at the upright position $x_1 = 3\pi,\ x_2 = 0$, the LQR controller would "unwind" the pendulum to bring it to $x_1 = x_2 = 0$.

3.1 Controllable targets

Under LQR control the linearized system is stable and we can solve the matrix Lyapunov equation [21] to find a Lyapunov function for this system

$$V = \mathbf{x}^{\mathrm{T}}\mathbf{P}\mathbf{x}, \quad \text{where} \quad \mathbf{P} = \begin{bmatrix} 1.3450 & 0.0283 \\ 0.0283 & 0.0627 \end{bmatrix}. \tag{3.3}$$

Since $\mathbf{P}$ is a positive definite matrix, lines of constant V are ellipses. We now seek the largest level curve $V = V_{\max}$ for which $\dot{V} < 0$ everywhere inside the ellipse using (3.1) under saturating LQR control. Since the problem is two dimensional, a value for $V_{\max}$ may be obtained by choosing a sufficiently small value for $V_{\max}$ so that integrating around the ellipse results in $\dot{V} < 0$ everywhere on this curve. A larger value for $V_{\max}$ may then be chosen and the process repeated until the inequality is satisfied with $\dot{V}$ very close to zero. Using this procedure results in $V_{\max} = 0.18$ for this problem. One advantage of this method for finding $V_{\max}$ is that it provides a numerical verification that the region inside the ellipse defined by (3.3) is a region of guaranteed asymptotic stability for the equilibrium point $x_1 = \pi,\ x_2 = 0$. The ellipse of Figure 3.2 is the one given by (3.3) with $V = V_{\max}$.

3.2 Chaotic attractor

In seeking an open loop control which will provide chaotic motion, it must be able to swing the pendulum to the upright vertical position from any given starting condition. An easy way to do this is to apply a sinusoidal voltage to the motor. For example, applying the control

$$u = 11 \cos 3t \tag{3.4}$$

will drive the system "over the top". This is a necessary but not a sufficient condition for chaos. While there are many amplitude-frequency combinations which will produce chaos, a small change in one of these values, may result in motion which is not chaotic [18]. It is not proven here that the control given by (3.4) does actually produce chaos. What is obtained may be a long chaotic transient [6] with the possibility that after a sufficiently long time period the trajectory could settle down to a limit cycle. However as long as (3.4) produces a long term chaotic transient (if not true chaos) over a range of starting conditions of interest, it remains a viable chaotic controller.

Given a sufficiently long running time, a chaotic controller will wind up the pendulum for many revolutions in both directions, moving past the origin many times in a random way as depicted in Figure 3.3. The small circles represent the location of the pendulum in state space at every 0.1 second. Clearly the chaotic attractor is very large in comparison with the controllable target just obtained. This implies that the waiting time between chaotic control and feedback control may be large. One way to improve the odds is to

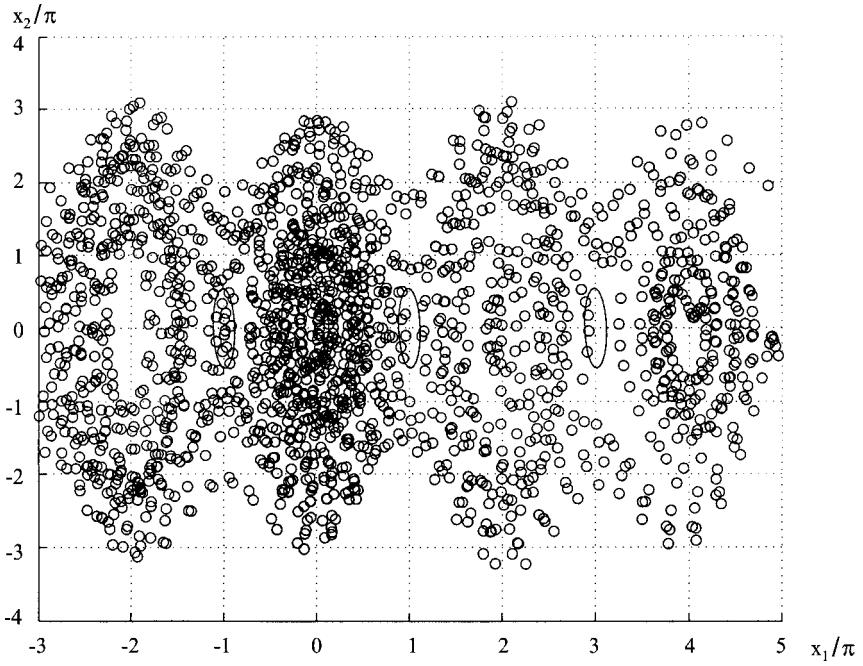

Figure 3.3. Chaotic attraction for the inverted pendulum.

simply increasing the number of targets. One obvious way of doing this is to introduce the ellipse just obtained at each of the points indicated by the stars in Figure 3.2. At each of these points the pendulum is in the upright position at zero velocity. The feedback control at these new targets must be adjusted accordingly. Three targets are illustrated in Figure 3.3. While the targets appear to have received many "hits" (especially the left one), there are only 21 points which lie inside the ellipses out of the 2,500 points (which lie inside the left/right limits of the figure and outside these limits). It should also be noted that the results shown in Figure 3.3 are only representative. It is possible that changing the initial conditions only slightly, using the same integration time, could result in more hits, no hits, or with most of the points lying outside the figure.

3.3 Intermediate targets

It is evident that it would be desirable to add additional targets. It has been previously shown that the waiting period required with the OGY method can be substantially reduced by using a "targeting method" [25]. This procedure uses intermediate targets in moving the system to a final target. We will use a similar procedure here. One way to arrive at additional intermediate targets is to simply integrate backward, under saturating LQR control from the neighborhood of the original equilibrium point $\bar{\mathbf{X}} = \begin{bmatrix} \pi & 0 \end{bmatrix}^{\mathrm{T}}$ using the initial conditions $\mathbf{x}(0) = \begin{bmatrix} \pi & \varepsilon \end{bmatrix}^{\mathrm{T}}$ and $\mathbf{x}(0) = \begin{bmatrix} \pi & -\varepsilon \end{bmatrix}^{\mathrm{T}}$ for a period of time, t_s. This results in two stopping points $\mathbf{x}_s^+$ and $\mathbf{x}_s^-$. At each of these stopping point we know that there exists some neighborhood about $\mathbf{x}_s^{\pm}$ such that if we integrate the system forward in time under saturating LQR control the system will be returned to $\bar{\mathbf{X}}$. Here we will choose t_s to be relatively small (e.g. so that the approximation $\sin x_1 = x_1$

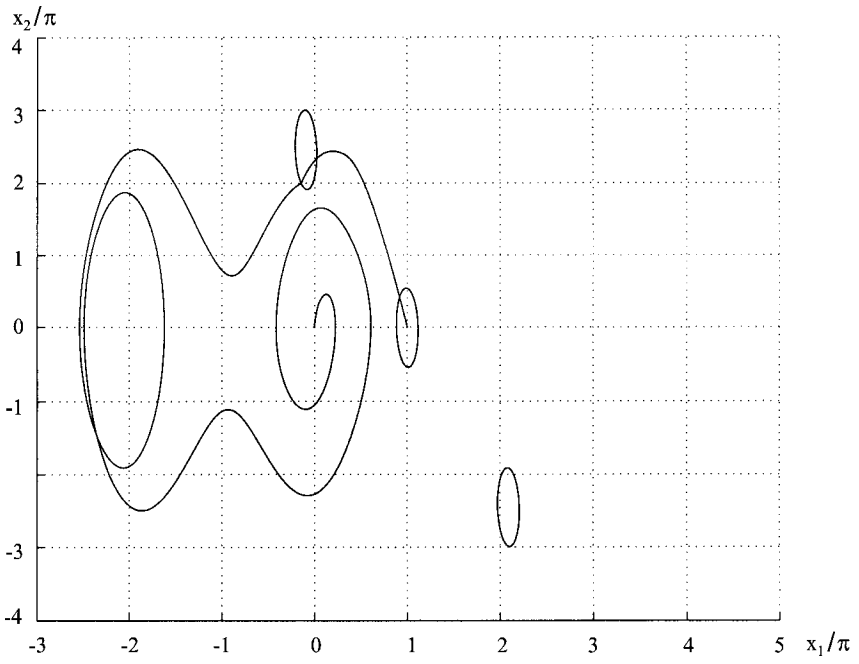

Figure 3.4. Utilizing chaos in the control of the inverted pendulum.

is valid) and use the controllable target ellipse centered at $\mathbf{x}_s^{\pm}$ to be an estimate of this additional neighborhood. If the system were indeed linear, the flow of all trajectories though the new intermediate target would converging to the line described by the retro trajectory. Unfortunately, for nonlinear systems there is no guarantee that all points in these intermediate targets will be controllable to the equilibrium point. This possibility does not defeat the method provided that we allow for it in the control algorithm. One way to do this is to make sure that chaotic control will be used in a small neighborhood of all equilibrium points other than the stars. In this way if the system enters a intermediate target, saturating LQR control is turned on, and the resultant trajectory does not arrive at a star, the chaotic control sequence will begin again. Clearly the majority of points in the intermediate target, under saturating LQR control must drive the system to a star in order for an intermediate target to be of any use.

A sample run using one control target at $\bar{\mathbf{X}}$ and two intermediate targets is illustrated in Figure 3.4. The system starts at the origin under (3.4) and remains under this control until it intersects the upper intermediate target. At this point saturating LQR control is applied which brings the system to $\bar{\mathbf{X}}$. In this case, since the chaotic trajectory is relatively short, it is shown as a solid line. Other example runs are similar and illustrate the usefulness of intermediate targets.

4 Bouncing Ball

A theoretical study of the motion of a ball bouncing on an oscillating plate is given in [26]. They construct an approximate map relating the velocity and phase between successive

impacts of a ball bouncing on an oscillating plate of infinite mass, and show that the motion of the ball can be chaotic, by demonstrating the existence of a horseshoe. For certain frequencies of the plate and certain initial conditions of the ball it is possible to get periodic motion for any integer period. Some of these periodic orbits are stable and some are not.

Two variables, the position of the plate and the time interval between bounces, can be used as state variables used to model the ball map. Each time the ball bounces on the plate there is an opportunity to measure the state of the system and apply a control. We will be controlling the frequency of the plate in order to achieve a specified objective for the motion of the ball. In particular, our objective is to position the ball so as to maintain the system at a specified fixed point of the ball map when the plate is moving at a specified nominal frequency $\bar{\omega}$.

The command frequency applied just after a bounce (at time t_j) is given by

$$\omega_j = \bar{\omega} + u_j$$

where u_j is the change in frequency from the nominal value. Between the last bounce and the next, therefore, the plate is controlled according to

$$y(t) = A\sin(\omega_j \tau + \phi_j) \tag{4.1}$$

where $y(t)$ is the displacement of the plate in the vertical direction, A is the amplitude of the plate, $\tau = t - t_j$, is time since the last bounce and

$$\phi_j = \omega_j(t_j - t_{j-1}) + \phi_{j-1}$$

is the phase angle of the plate at the time of the last bounce. For this situation, it is not difficult to show that under the assumption that the bounce height is large compared to A, that the ball map is given by [27]

$$\begin{aligned} \phi_{j+1} &= \phi_j + \frac{\omega_j}{\bar{\omega}}\,\psi_j, \\ \psi_{j+1} &= -a_2\psi_j + \hat{a}_1\bar{\omega}\omega_j\,\cos\phi_{j+1}, \end{aligned} \tag{4.2}$$

where ψ_j is the change in phase between bounces (related to the time interval between bounces) a_2 and $\hat{a}_1$ are constants whose values depend on the mass ratio of the ball to the plate, the coefficient of restitution, the amplitude of the plate, and the acceleration of gravity.

When equations (4.2) are iterated to produce a dynamical solution, the first equation is evaluated modulo 2π since ϕ refers to a physical position of the plate. The second equation is not evaluated modulo 2π since the plate may go through more than one cycle before the next bounce.

There are many possible periodic solutions to (4.2). For example the ball can bounce to a fixed height at every n cycles of the plate. It can also bounce to m different heights at $n \times m$ cycles of the plate before repeating the pattern.

Figure 4.1 shows some of the kinds of dynamics possible with an actual bouncing ball system. In the top figure, the initial conditions were set very close to those corresponding to an unstable period-1 solution. We see the ball diverge from this solution and approaches a stable period-2 solution corresponding to $m = 2,\ n = 1$. In the middle

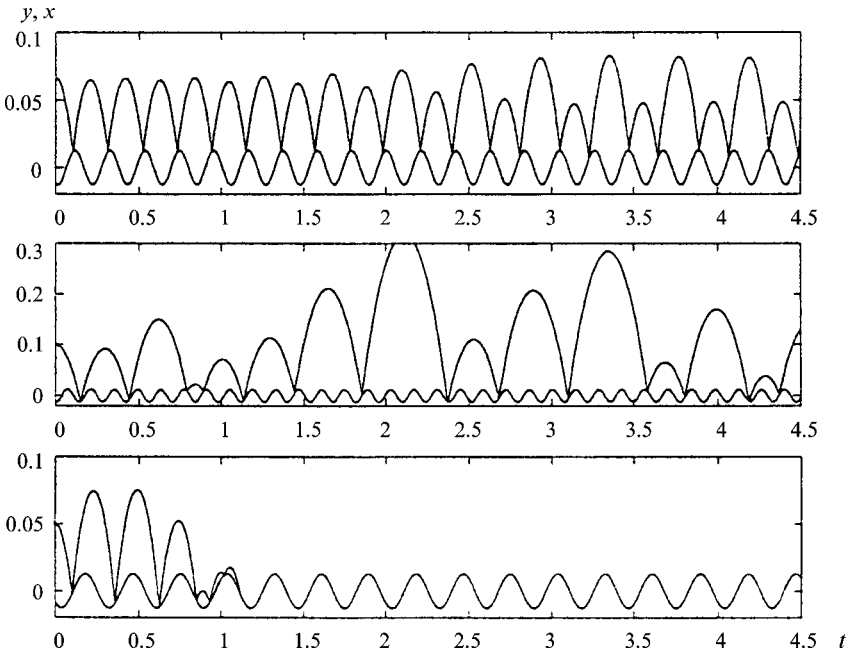

Figure 4.1. Ball and plate motion. (top) A stable period-2 solution at $\omega = 30$ rad/sec. (middle) Chaotic motion at $\omega = 45$ rad/sec. (bottom) The ball can ride on the plate when $\omega = 22$ rad/sec.

figure, the ball bounces chaotically, with different n values between different steps. In the bottom figure, the plate frequency is such that a stable period one solution exists, however in this case, the initial conditions are not near this solution and the ball ends up riding on the plate after a few bounces.

4.1 Chaotic attractor

For the experimental bouncing ball system located at the University of Arizona non-linear control system laboratory, the parameters are given by $a_2 = -0.733$ and $\hat{a}_1 = 0.00459$. With these values, it turns out that the high-bounce map (4.2) produces chaotic motion with $\bar{\omega} = 45$ rad/sec as shown in the middle illustration of Figure 4.1. Figure 4.2 illustrates the corresponding chaotic attractor. The map was obtained by starting the system at $\phi(0) = 0$ and $\psi(0) = 9.1743$ radians and run for 1000 iterations. The values of ϕ and ψ are divided by 2π before plotting. The resulting chaotic attractor lies between an upper and lower bound as indicated in the figure. The upper bound is related to the height the ball would bounce, if it could bounce periodically at the phase angle ϕ and the lower bound is related to the height the ball would achieve if were to impact the plate at the phase angle ϕ with zero velocity. Under the high-bounce map (4.2) negative values for ψ are possible (corresponding to a negative bounce height). Since this is not physically possible, a slight modification of the map was used to produce Figure 4.2. Details of this modification are discussed in [17].

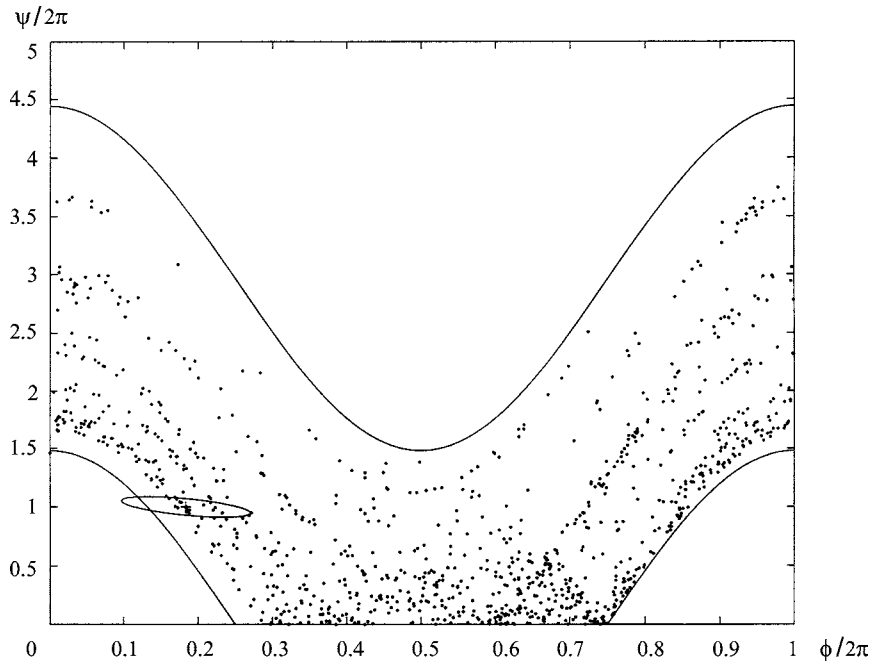

Figure 4.2. Chaotic attractor for the high-bounce map when $\omega = 45$ rad/sec.

4.2 Feedback controllers for the ball

We will consider only one case with $m = n = 1$ for a bounce pattern that is unstable in the absence of control.

We seek fixed point solutions (with $\omega_j = \bar{\omega}$) for

$$\begin{aligned} \bar{\phi} &= \bar{\phi} + \bar{\psi}, \\ \bar{\psi} &= -a_2\bar{\psi} + \hat{a}_1\bar{\omega}^2 \cos(\bar{\phi} + \bar{\psi}). \end{aligned} \tag{4.3}$$

In order to obtain equilibrium solutions from (4.3) the right hand side of the first equation must be evaluated modulo 2π, in which case we obtain

$$\begin{aligned} \bar{\psi} &= 2\pi, \\ \cos\bar{\phi} &= \frac{2\pi(1 + a_2)}{\hat{a}_1\bar{\omega}^2}. \end{aligned} \tag{4.4}$$

In order to design an LQR feedback controller, it is assumed that system is near enough to the fixed point to so that the motion may be approximated by a linear map. Let

$$\begin{aligned} x_1 &= \phi - \bar{\phi}, \\ x_2 &= \psi - \bar{\psi} \end{aligned}$$

be perturbations in ϕ and ψ from the nominal values given by (4.4) and let

$$u = \omega - \bar{\omega}$$

be a perturbation in frequency from the nominal value $\bar{\omega}$. First order changes in (4.2) are given by

$$x_{1_{j+1}} = x_{1_j} + \frac{\omega_j}{\bar{\omega}}\, x_2 + \frac{\psi_j}{\bar{\omega}}\, u_j,$$
$$x_{2_{j+1}} = -\hat{a}_1 \bar{\omega}\omega_j \sin\phi_j x_{1_{j+1}} - a_2 x_{2_j} + \hat{a}_1 \bar{\omega} \cos\phi_{j+1} u_j.$$

Evaluating these equations at $\omega_j = \bar{\omega},\ \psi_j = \bar{\psi},\ \phi_j = \bar{\phi}$, and $\phi_{j+1} = \bar{\phi} + \bar{\psi}$, results in

$$\mathbf{x}_{j+1} = \mathbf{A}x_j + \mathbf{B}u_j$$

with

$$\mathbf{A} = \begin{bmatrix} 1 & 1 \\ a_{21} & -a_2 + a_{21} \end{bmatrix} \qquad \mathbf{B} = \begin{bmatrix} \frac{\bar{\psi}}{\bar{\omega}} \\ a_{21}\frac{\bar{\psi}}{\bar{\omega}} + \hat{a}_1\bar{\omega}\cos\bar{\phi} \end{bmatrix},$$

where $a_{21} = -\hat{a}_1\bar{\omega}^2 \sin\bar{\phi}$.

The LQR method for discrete systems may now be applied [23]. Once the gains have been determined by this process the system is controlled by adjusting the frequency every time the ball bounces according to

$$\omega = \bar{\omega} - k_1(\phi - \bar{\phi}) - k_2(\psi - \bar{\psi}). \tag{4.6}$$

4.3 Ball under control

With a plate frequency of $\bar{\omega} = 30$ there is an unstable period-1 $(m = 1,\ n = 1)$ solution to the high-bounce map, with $\bar{\phi} = 1.154$ and $\bar{\psi} = 2\pi$. The eigenvalues have magnitudes -0.4625 and -1.5855, so the solution is unstable. This is shown in the top illustration of Figure 4.1 where the initial condition was chosen very close to the fixed point solution. We see in this case that while the period-1 solution is unstable, the period-2 solution corresponding to $\bar{\omega} = 30$ is obviously stable. Our objective in this case is to stabilize the unstable solution.

The linearization of the high-bounce map results in

$$\mathbf{A} = \begin{bmatrix} 1 & 1 \\ -3.780 & -3.047 \end{bmatrix} \qquad \mathbf{b} = \begin{bmatrix} 0.2094 \\ -0.7358 \end{bmatrix}.$$

Using LQR design with $\mathbf{Q} = \mathbf{I},\ R = 1$, the MATLAB command **dlqr** results in the feedback gains

$$\mathbf{k} = \begin{bmatrix} 3.931 & 2.843 \end{bmatrix}$$

with eigenvalues for the controlled system $\bar{\mathbf{A}} = \mathbf{A} - \mathbf{B}\mathbf{k}$ given by

$$\lambda = -0.3890 \pm 0.1975i \quad (|\lambda| = 0.4363)$$

all of which demonstrates that the system is locally asymptotically stable. Thus there must exist a 2×2 symmetric positive definite solution for $\mathbf{P}$ satisfying the discrete Lyapunov equation

$$\mathbf{P} = \hat{\mathbf{Q}} + \mathbf{A}^{\mathrm{T}}\mathbf{P}\mathbf{A},$$

where $\hat{\mathbf{Q}}$ is any 2×2 symmetric positive definite matrix such that

$$V = \mathbf{x}^{\mathrm{T}}\mathbf{P}\mathbf{x}$$

is a Lyapunov function for the system. Choosing $\hat{\mathbf{Q}} = \mathbf{I}$, we obtain

$$\mathbf{P} = \begin{bmatrix} 2.6290 & 1.5560 \\ 1.5560 & 2.5834 \end{bmatrix}.$$

Finding the largest V for which $\dot{V} < 0$ around a constant V contour results in $V_{\max} = 0.5$. This is the elliptical level curves illustrated in Figure 3.3. A small "+" locates the equilibrium solution.

5 Discussion

The procedures used here have actually been used to control both the inverted pendulum and the bouncing ball and have resulted in very satisfactory performance [16]. The bouncing ball is the more difficult system to control and it was found that due to inaccuracies in measuring ϕ and ψ, a somewhat larger value of $V_{\max}$ needs to be used. As a consequence, from time to time, the ball is not captured when the closed-loop feedback control is turned on. However the overall performance is quite satisfactory. The system is always started with the ball at rest on the plate. Generally fewer bounces under the $\omega = 45$ rad/sec control are needed to enter a controllable target than might be expected from the ball map results illustrated in Figure 4.2.

References

[1] Poincaré, H. (1892). *Les Méthodes Nouvelles de la Méchanique Celeste*. Gauthier-Villars, Paris. In English: NASA Translation TTF-450/452, U.S. Federal Clearinghouse, Springfield, VA, 1967.

[2] Lorenz, E.N. Deterministic non-periodic flow. *J. Atmos. Sci.* **20** (1963) 130–141.

[3] May, R.M. Simple mathematical models with very complicated dynamics. *Nature* **261** (1976) 459–467.

[4] Ott, E., Grebogi, C. and York, J.A. Controlling chaos. *Physical Review Letters* **64** (1990) 1196–1199.

[5] Chen, G and Dong, X. Control of Chaos – A Survey. *Proceedings of the 32nd "IEEE Control and Decision" Conference*, San Antonio Texas, Dec. 15-17, 1993.

[6] Vincent, T.L. and Yu, J. Control of a chaotic system. *Dynamics and Control* **1** (1991) 35–52.

[7] Chen, G and Dong, X. From chaos to order – perspectives and methodologies in controlling chaotic nonlinear dynamical systems. *International Journal of Bifurcation and Chaos* **3**(6) (1993) 1363–1409.

[8] Hartley, T. and Mossayebi, F. A classical approach to controlling the Lorenz equations. *International Journal of Bifurcation and Chaos* **2**(4) (1992) 881–887.

[9] Paskota, M., Mees, A.I. and Teo, K.L. Stabilizing higher periodic orbits. *International Journal of Bifurcation and Chaos* **4**(2) (1994) 457–460.

[10] Paskota, M., Mees, A.I. and Teo, K.L. *On Local Control of Chaos, the Neighborhood Size*. Manuscript, personal communication, 1995.

[11] Judd, K., Mees, A., Teo, K.L. and Vincent, T.L. *Control and Chaos*. Birkhäuser, Boston, 1997.
[12] Tél, T. Controlling transient chaos. *J. Phys. A: Gen.* **24** (1991) L1359–L1368.
[13] Alvarez, J. Nonlinear regulation of a Lorenz system by feedback linearization techniques. *Dynamics and Control* **4** (1994) 277–298.
[14] Singer, J., Wang, Y.Z. and Bau, H.H. Controlling a chaotic system. *Physical Review Letters* **66**(9) (1991) 1123–1125.
[15] Vincent, T.L., Schmitt, T.J. and Vincent, T.L. A chaotic controller for the double pendulum. In: *Mechanics and Control*. (Ed.: R.S.Guttalu), Plenum Press, New York, (1994) 257–273.
[16] Vincent, T.L. Controllable targets near a chaotic attractor. In: *Control and Chaos*, (Eds.: by K.Judd, A.Mees, K.L.Teo, and T.L.Vincent), Birkhäuser, Boston, 1997.
[17] Vincent, T.L. Control using chaos. *IEEE Control Systems* **17**(6) (1997) 65–76.
[18] Schuster, H.G. *Deterministic Chaos, An Introduction*. VCH, Weinheim, 1988.
[19] Leitmann, G. *An Introduction to Optimal Control*. McGraw-Hill, New York, 1966.
[20] Bryson, A.E. and Ho, Y.C. *Applied Optimal Control*. Blaisdell, Waltham, Massachusetts, 1969.
[21] Vincent, T.L. and Grantham, W.J. *Nonlinear and Optimal Control Systems*. Wiley, New York, 1997.
[22] Goh, C.J. and Teo, K.L. *MISER: An Optimal Control Software, Theory and User Manual*. Industrial and Systems Engineering, National University of Singapore, Singapore, 1987.
[23] Ogata, K. *Discrete-Time Control Systems*, Prentice Hall, Englewood Cliffs, New Jersey, 1987.
[24] Ogata, K. *Modern Control Engineering*. Prentice Hall, Englewood Cliffs, New Jersey, 1997.
[25] Kostelich, E.J. and Barreto, E. Targeting and control of chaos. *Control and Chaos*. (Ed.: K.Judd, A.Mees, K.L.Teo, and T.L.Vincent), Birkhäuser, Boston, 1997.
[26] Guckenheimer J. and Holmes, P. *Nonlinear Oscillations, Dynamical Systems and Bifurcations of Vector Fields*. Springer-Verlag, New York, 1983.
[27] Vincent. T.L. and Mees, A.I. Controlling a bouncing ball. *Journal of Bifurcation and Chaos* **10**(3) (2000) 579–592.